Triblock copolymer templated semi-crystalline mesoporous titania films containing emulsion-induced macropores

Xiangju Meng, Tatsuo Kimura,* Tatsuki Ohji and Kazumi Kato

Received 30th August 2008, Accepted 5th January 2009
First published as an Advance Article on the web 11th February 2009
DOI: 10.1039/b815165b

Triblock copolymer templated synthesis of titania films in water (without ethanol) was demonstrated, which led to the formation of emulsions in the aqueous precursor solutions by adding hydrophobic 1,3,5-triisopropylbenzene (TIPBz). A cubic *Im*-3*m* mesoporous anatase film containing emulsion-induced macropores was prepared by spin-coating of an aqueous precursor solution of water-soluble triblock copolymer such as Pluronic F127 through the evaporation-induced self-assembly approach. The addition of TIPBz in the aqueous system also affords pinhole-like macrospaces in the mesostructured film. Expansion of the pinhole-like macrospaces during calcination would offset a tensile stress through shrinkage with the retention of the mesostructure, leading to complete crystallization of the titania framework that is important for effective adsorption of DNA molecules.

1. Introduction

Mesoporous materials have drawn much attention because of their specific features such as high surface area, large adsorption capacity, and tunable mesopores as well as the controllable composition of the frameworks and the morphology.[1–4] Mesoporous films of transition metal oxides such as titania are greatly important for both fundamental research and practical application as devices in fields such as optics, sensors, catalysts, and electronics. Since the synthesis of lamellar mesostructured titania films using alkyltrimethylammonium surfactants,[5] a wide variety of mesoporous titania films have been prepared using nonionic and polymeric surfactants such as poly(oxy ethylene) alkyl ether[6–9] and poly(oxyethylene)-*block*-poly(oxypropylene)-*block*-poly(oxyethylene) triblock copolymer ($EO_nPO_mEO_n$).[8–16] Ordered mesoporous titania films have mainly been synthesized through evaporation-induced self-assembly of triblock copolymer molecules interacting with inorganic species in ethanol (containing a small amount of water) strongly acidified by the addition of hydrochloric acid to hydrolyzed titanium alkoxides and/or by using $TiCl_4$ as a starting titania source.[6–16]

Titania frameworks can be crystallized partly by heating; anatase nanocrystals are formed within pore walls of EO_nPO_m-EO_n-templated materials.[9–16] However, the crystallinity of the titania frameworks around ordered mesopores reported so far was not satisfactory because the ordered mesostructures collapsed through complete crystallization of the frameworks caused by thermal treatment at higher temperatures. Transformation of amorphous titania phase to anatase occurs at around 400 °C.[17,18] Although it has been reported that post-treatment with silicon or titanium alkoxide in supercritical carbon dioxide is useful for improving mesostructural stability,[19,20] full crystallization of titania frameworks by facile methods has been demanded for intelligent uses of mesoporous titania films in photovoltaic cells,[21] photocatalysts,[22–27] self-cleaning films,[28] dye-sensitized solar cells,[29–32] optical waveguides and interferometric chemical sensors.[33]

Several excellent examples for full crystallization of titania frameworks have been reported so far.[34–38] Grosso *et al.* reported that a cubic *Im*-3*m* derived (*R*-3*m*) mesoporous film with fully nanocrystallized anatase frameworks was obtained by carefully delayed rapid crystallization, stable up to 700 °C.[34] Thermally driven densification, pyrolysis, crystallization, and sintering of ordered mesoporous titania films was elucidated by *in-situ* thermal ellipsometric analysis.[35] Smarsly *et al.* have synthesized cubic *Im*-3*m* and 2-D hexagonal (*p*6*mm*) mesoporous titania films with controlled crystallinities using a unique block copolymer called KLE.[36,37] The use of KLE induced the formation of thick amorphous walls, resulting in the retention of the mesostructures after complete crystallization of the titania frameworks. Mesostructured film with thick titania walls was also obtained from controlled titania precursors in the presence of Pluronic F127 ($EO_{106}PO_{70}EO_{106}$), resulting in crystallization of the frameworks.[38] Wu *et al.* found an interesting structural transformation of a 3-D hexagonal ($P6_3/mmc$) mesostructured titania film prepared using Pluronic P123 ($EO_{20}PO_{70}EO_{20}$) in ethanol into a mesoporous film constructed by hexagonally arranged anatase pillars.[39] The preparation of a mesoporous titania film was also possible in a similar manner by using Pluronic F127 without water.[40] It has also been reported that the thermal stability of mesostructured titania films is strongly influenced by the surface structures of substrates.[41]

Fabrication of ordered porous titania films at multiple length scales is important technology for minute creation of porous devices advantageous for diffusion, separation, and transport of large organic molecules.[42,43] Crystallinity of titania frameworks of such porous materials should also be increased for practical applications of such porous films to high-performance electrodes and highly active photocatalysts, and thus the preparation of titania films with both crystalline framework and hierarchical

Advanced Manufacturing Research Institute, National Institute of Advanced Industrial Science and Technology (AIST), Shimoshidami, Moriyama-ku, Nagoya, 463-8560, Japan. E-mail: t-kimura@aist.go.jp

mesoporous–macroporous structure is one of the most challenging topics. Uniform latex particles such as polystyrene (PS) beads have often been used to accommodate ordered macropores inside particles,[44–46] but ordered mesoporous–macroporous titania films have not been obtained yet because latex particles preferentially aggregate one another and then it is difficult to form mesostructured products between the PS particles. Accordingly, emulsion templating is very attractive and challenging for affording macroporous materials[47] because surfactant molecules are homogeneously present at the interfaces between water and oil, possibly leading to the formation of mesostructured products between emulsions.

All of the syntheses of mesoporous titania films using surfactants such as triblock copolymers reported so far have been conducted in ethanolic solutions,[6–16] concluding that emulsions are not formed in such solutions even after the addition of hydrophobic organic solvents. Accordingly, a water-soluble triblock copolymer, Pluronic F127, was used here as a surfactant and then the synthesis was performed in an aqueous system. Therefore, in the present study, we succeeded in demonstrating a facile and one-pot method to prepare an ordered semi-crystalline mesoporous titania film containing emulsion-induced macropores, which will extend applications based on ordered porous titania films. The formation of such macropores in the cubic *Im*-3*m* mesostructured titania film was caused by the addition of 1,3,5-triisopropylbenzene that played an important role as an oil in water. This will subsequently lead to the further design of mesostructured and mesoporous titania films using water-soluble organic dyes and organometallic complexes, as well as metal ions,[48–51] and metals[53,54] for potential applications. Immobilization of a wide variety of proteins has already been investigated by many research groups.[55] However, all of the studies have been focused on ordered mesoporous silicas,[55] and thus it is quite important for further design of porous materials to understand adsorption of biomolecules over non-silica-based materials. Actually, we investigated adsorption of DNA molecules over mesoporous titania films, possibly affording novel nano-devices applicable to not only dye-sensitized solar cells but also highly selective sensors of toxic organic molecules using attached DNA molecules at the titania surfaces.

2. Experimental

2.1 Materials

Titanium tetraisopropoxide (TTIP), concentrated hydrochloric acid (35.5% HCl), and an aqueous solution of HCl (5M) were purchased from Wako Chemical Co. TTIP was used without further purification. Water-soluble triblock copolymer (Pluronic F127, $EO_{106}PO_{70}EO_{106}$) and aqueous solutions of polystyrene beads with the diameters of 100, 300, and 900 nm (10 mass%) were obtained from Aldrich. Organic additives, for example 1,3,5-triisopropylbezene (TIPBz), were obtained from Lancaster. Silicon (p-type [100]) and F-doped tin oxide (FTO) substrates were purchased from High Purity Chemical Co. and Asahi Glass Co., respectively. The substrates were cleaned by a UV-ozone treatment (SEN LIGHTS Co. Photo Surface Processor PL16-110) for 15 min before spin-coating.

2.2 Synthesis of *Im*-3*m* mesoporous titania films using Pluronic F127 in water

According to the literature describing the synthesis of titania in ethanol using Pluronic P123,[39] we optimized the synthesis parameters in an aqueous system using Pluronic F127 carefully. In a typical synthesis, 0.74 mL of 35.5% HCl was added very slowly to 1.35 g of TTIP under vigorous stirring. After stirring for 10 min, the hydrolyzed solution was mixed with 3 mL of 5M HCl containing 0.2 g of Pluronic F127 and 0.6 g of TIPBz. After stirring for another 15 min, the resultant aqueous solution, which was not homogeneous, was spin-coated on cleaned FTO and Si substrates with a spinning rate of 3000 rpm. The as-coated films were aged at −20 °C over 1 h, dried at 50 °C for 1 h, and calcined at temperatures of 250–500 °C with a heating rate of 1 °C min^{-1} for 3 h. A homogeneous aqueous solution was obtained without TIPBz in a similar manner. The as-made films were heated to 250 and 400 °C with a heating rate of 1 °C min^{-1} in flowing N_2 and maintained at these temperatures for 1 h, followed by calcination at these temperatures for another 2 h in flowing O_2.

2.3 Adsorption of DNA molecules over mesoporous titania films

An aqueous solution of DNA molecules labeled with cytochrome (100 nM) was dropped onto mesoporous titania films and then allowed to be permeated at 95 °C for 10 min. The resultant films were washed three times with an aqueous solution of sodium dodecylsulfate (0.2%) for 15 min, rinsed with ultrapure water, and immersed in boiling water for 2 min and in dehydrated ethanol at 4 °C for 1 min. Adsorption of the DNA molecules was checked by excitation-emission fluorescence (GE Healthcare UK Ltd. Typhoon Trio scanner) from the attached cytochrome. Intensity PMT580 (in Fig. 12) means a relative intensity range of 655–685 nm from the dye molecule exited by irradiation at 633 nm.

2.4 Characterization

Powder X-ray diffraction (XRD) patterns were recorded on a Rigaku RINT 2100 diffractometer with monochromated Fe Kα radiation. Transmission electron microscopic (TEM) images were taken by a JEOL JEM 2010, operated at 200 kV. The TEM images were taken by using powders scratched off from calcined films on FTO. Scanning electron microscopic (SEM) images were taken by JEOL JSM6335-FM and HITACHI S-4700. Kr adsorption–desorption isotherms were obtained by using a Quantachrome Autosorb-1 at 87 K (liquid Ar). Calcined films on Si with a total area of *ca.* 100 cm^2 were introduced into an exclusive sample cell and degassed at room temperature under vacuum before the measurements. If the density of titania frameworks calcined at 400 °C is 4.0 g cm^{-3} (anatase), the sample weight can be calculated by using the pore volume and the average film thickness (measured by using a KLA-Tencor P-15 surface profiler) and then the BET surface area is roughly calculated by using those values. N_2 adsorption–desorption isotherms were obtained by using the same apparatus at 77 K in order to elucidate the BET surface area and pore size distribution. Powder samples were recovered by scratching off from a large number of as-made films on Si and then calcined at 400 °C

very slowly, and degassed at 110 °C for 6 h under vacuum prior to the measurement.

3. Results and discussion

3.1 Synthesis of *Im*-3*m* mesoporous titania films using F127 in water

The transmission electron microscopic (TEM) images of mesoporous titania films prepared without TIPBz and calcined at 250 and 400 °C are shown in Fig. 1. A typical image along the [100] direction associated with a body-centered cubic space group (*Im*-3*m*) can be seen clearly. It was confirmed that the titania frameworks were amorphous after calcination at 250 °C. The ordered mesostructure disappeared after calcination at 400 °C and nanocrystals with the particle size of *ca.* 10 nm were observed over the entire film, as reported previously.[22–24] A high-magnification image of the titania film calcined at 400 °C is shown in Fig. 2. Lattice fringes due to anatase phase were observed throughout the nanoparticles that surrounded intercrystalline mesospaces (*ca.* 10 nm). The results indicate that cubic *Im*-3*m* mesostructured titania film is thermally unstable and the mesostructure collapses by grain growth of the titania frameworks.

The Kr adsorption–desorption isotherms of the mesoporous titania films are shown in Fig. 3. Both isotherms were type IV, typical for mesoporous materials, while capillary condensation started at different relative pressures (P/P_0). If the density of calcined titania frameworks is 4.0 g cm^{-3} (anatase phase), the BET surface areas of the mesoporous titania films calcined at 250 and 400 °C are roughly calculated to be *ca.* 99 m^2 g^{-1} (283 m^2 cm^{-3}) and 122 m^2 g^{-1} (331 m^2 cm^{-3}), on the basis of the pore volumes (0.28 cm^3 cm^{-3} and 0.32 cm^3 cm^{-3}), respectively. However, the surface area of the film calcined at 250 °C is

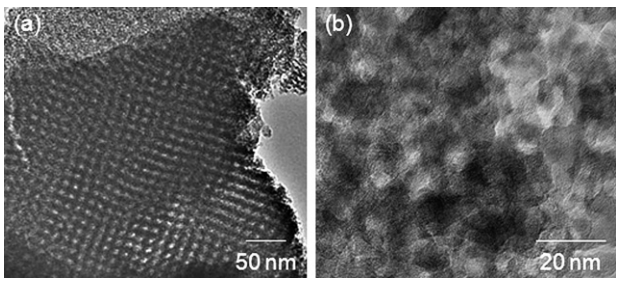

Fig. 1 TEM images of mesoporous titania films prepared using F127 in water (without TIPBz), followed by calcination at (a) 250 °C and (b) 400 °C.

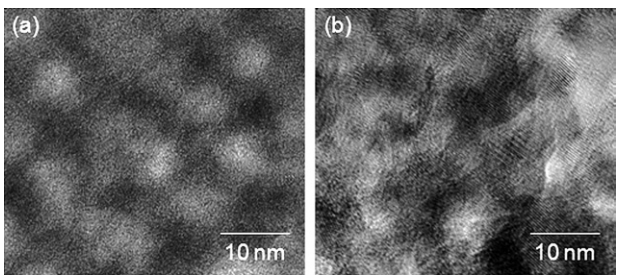

Fig. 2 High-resolution TEM images of Fig. 1.

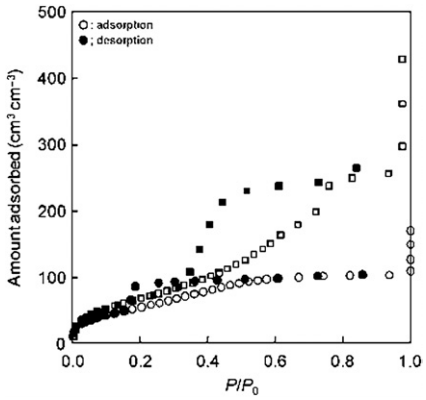

Fig. 3 Kr adsorption–desorption isotherms at 87K of mesoporous titania films prepared using F127 in water (without TIPBz), followed by calcination at (○) 250 °C and (□) 400 °C.

underestimated because the density of amorphous titania phase must be smaller than that of anatase. As proved by TEM (Fig. 1a), the cubic *Im*-3*m* mesostructure was retained after calcination at 250 °C. According to the presence of cage-type uniform mesopores, a clear H2 hysteresis loop was observed in the Kr isotherm. The mesostructure was not maintained after calcination at 400 °C, but intercrystalline mesospaces were formed in the film (Fig. 1b). Accordingly, a type IV isotherm was observed with a loose hysteresis loop and capillary condensation started at P/P_0 higher than that observed for the film calcined at 250 °C.

3.2 Synthesis of *Im*-3*m* mesoporous titania film using F127 in water with TIPBz

Thermal stability of cubic *Im*-3*m* mesostructured titania film was drastically improved by the addition of TIPBz to the precursor solution. The X-ray diffraction (XRD) patterns and TEM images of as-made and calcined films are shown in Fig. 4 and 5, respectively. The XRD pattern of the as-made film exhibited three peaks in the range of 1.0–2.5° (Fig. 4a), assignable to (110), (200), and (211) reflections of a cubic *Im*-3*m* mesostructure.[42,43] The TEM images also showed the formation of the cubic *Im*-3*m* mesostructure (Fig. 5a–c). The XRD patterns of the mesoporous

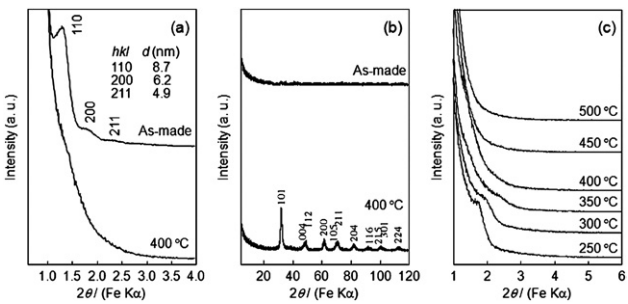

Fig. 4 (a) XRD patterns of the titania films before and after calcination at 400 °C at low diffraction angles, (b) those of the corresponding powder samples, recovered by scratching off the films on Si and then calcined at 400 °C, at high diffraction angles, and (c) XRD patterns of the titania films calcined at various temperatures at low diffraction angles.

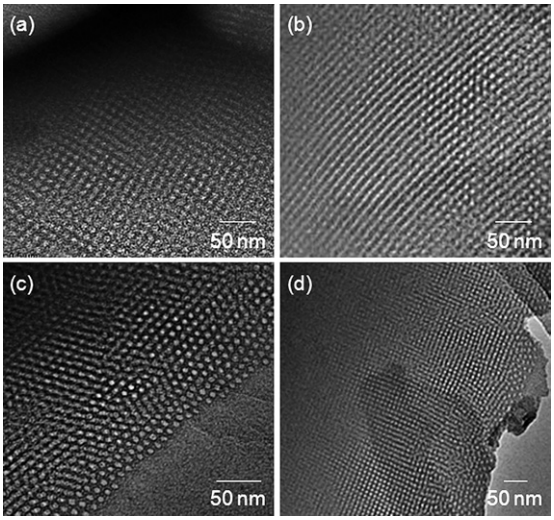

Fig. 5 TEM images of (a) [100], (b) [110], and (c) [111] directions of as-made film with a cubic *Im*-3*m* mesostructure and (d) the film calcined at 400 °C.

films calcined at 250–350 °C exhibited broad peaks at low diffraction angles with decreasing intensity, which disappeared after calcination above 400 °C (Fig. 4c), which was attributed to gradual distortion of the titania frameworks by crystallization to anatase and/or slight grain growth. However, the TEM image of the film calcined at 400 °C still showed the presence of an ordered mesostructure even after calcination (Fig. 5d), which was reproducible. It is considered that the calcined film does not contain any long-range orderings that may be distorted by the variation of macropores/macrospaces during calcination with the crystallization of titania frameworks, and so we are now investigating that directly by careful XRD of the films. The cubic *Im*-3*m* mesostructure was transformed into regularly arranged pillars by grain growth during calcination at 500 °C (Fig. 6), suggesting a grid-like transformation promoted by crystallization and diffuse sintering of amorphous titania to anatase starting between 400 and 500 °C.[34,52]

A high-resolution TEM image of the film calcined at 400 °C revealed that the whole frameworks were crystallized with the retention of the cubic mesostructure (Fig. 7). The thicknesses of the as-made film (*ca.* 900 nm) decreased to *ca.* 600 nm upon calcination. The selected area electron diffraction (SAED) pattern showed diffraction rings characteristic of randomly oriented small domains of anatase crystals. A series of the rings are assignable to peaks typically observed for anatase-type

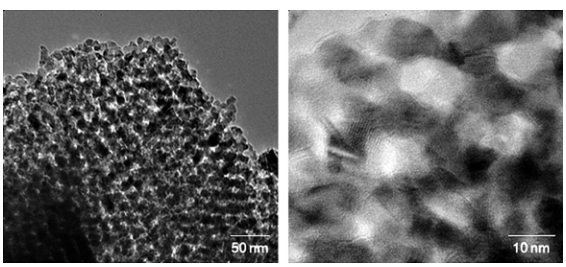

Fig. 6 TEM images of the film calcined at 500 °C.

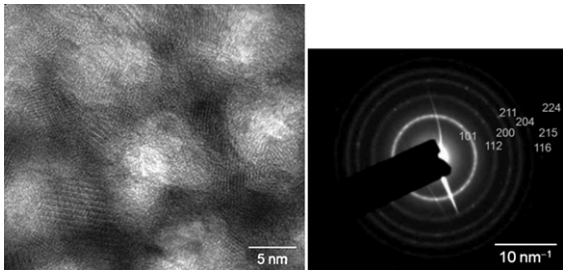

Fig. 7 High-resolution TEM image of the film calcined at 400 °C with corresponding SAED pattern.

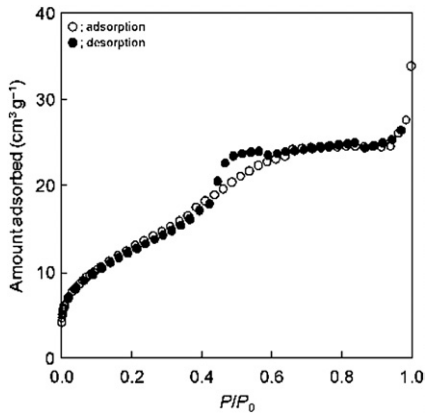

Fig. 8 N_2 adsorption–desorption isotherm of the corresponding powder sample calcined at 400 °C.

titania crystals without rutile and brookite. The XRD pattern of the powder sample calcined at 400 °C also supported the formation of anatase crystals (Fig. 4b). All of the results suggested that the titania film was composed of crystallized anatase nanoparticles around ordered mesopores. The N_2 adsorption–desorption isotherm of the corresponding powder sample, which was recovered by scratching off from Si substrates, showed type IV behavior with a H2 hysteresis loop (Fig. 8), characteristic of porous materials with cage-type uniform mesopores.[56,57] It is quite arguable to elucidate the pore sizes of cage and window on the basis of the N_2 adsorption data, because adsorption behavior of gas on cage-type mesopores (cavitation, pore blocking, etc.) is totally different from that on cylindrical mesopores.[58,59] The lower closure pressure in cage-type mesopores does not depend on the cage size[60] which was calculated on the basis of the nonlocal density functional theory. The window size of cage-type mesopores was indirectly estimated by a method to check pore opening by N_2 adsorption after organic modification.[61,62] The BET surface area was 52 m^2 g^{-1}, which is lower than those observed for the aforementioned films prepared without TIPBz as well as a previously reported one.[34] This is probably related to the presence of macropores in the film (see Scheme 2 later).

3.3 Formation of emulsion-induced macropores in mesostructured titania films prepared using F127 in water with TIPBz

The TEM image of an as-made film is shown in Fig. 9, exhibiting the presence of large pores. Such macropores, whose possible

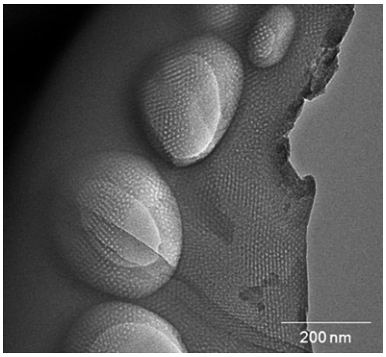

Fig. 9 TEM image of the as-made film before calcination.

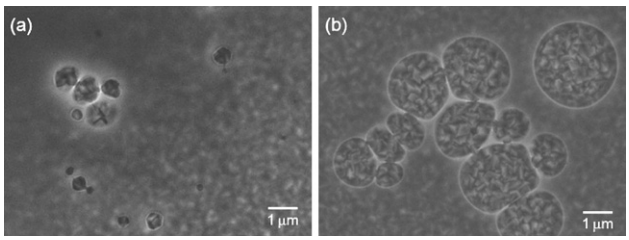

Fig. 10 SEM images of the films (a) before and (b) after calcination at 400 °C.

formation mechanism is described below, with the diameter of 0.1–1 μm are connected through the ordered mesopores in the cubic arrays. The scanning electron microscopic (SEM) images of as-made and calcined films are shown in Fig. 10, revealing the presence of another type of macrospace that look like pinholes (0.1–5 μm) because uneven surfaces of F-doped tin oxide (FTO) were observed distinctly. Interestingly, it was confirmed that the macrospaces were expanded during calcination.

Further investigation of the synthesis conditions was carried out in order to confirm the role of TIPBz to introduce macropores and pinhole-like macrospaces in the mesostructured titania films. Such macropores and pinholes were not formed without TIPBz and other organic auxiliary additives such as 1,3,5-trimethylbenzene were not useful for affording macropores and pinholes, though ordered mesostructured titania films can be

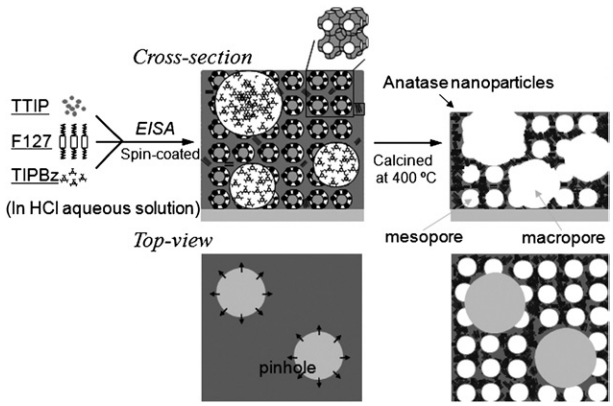

Scheme 1 Schematic formation mechanism of semi-crystalline mesoporous titania film containing macropores.

obtained in the presence of Pluronic F127. The results suggest an important role of TIPBz in the formation of macropores and pinholes. Pinhole-like macrospaces would be formed by phase separation in water when an excess amount of TIPBz is present in the reaction system. Strongly hydrophobic TIPBz is undissolved in water, but slightly dissolved in isopropanol derived from the hydrolysis of TTIP. The amount of TIPBz solubilized in isopropanol should be controlled very carefully to keep the suitable amount of undissolved TIPBz in the heterogeneous system. Eventually, macroscale spaces occupied by indissoluble TIPBz like emulsions are formed by evaporation of solvents while spin-coating (Scheme 1).

3.4 Role of macropores in forming semi-crystalline mesoporous titania films

A cubic *Im*-3*m* mesoporous titania film without macropores was not thermally stable and the mesostructure disappeared with grain growth of titania frameworks during calcination at 400 °C and then anatase nanocrystals with the particle size of *ca.* 10 nm were formed over the entire film (section 3.1). Interestingly, the mesostructure was maintained even after calcination at 400 °C in the presence of macropores (sections 3.2 and 3.3). It was found that the film contained two types of large pores (called emulsion-induced macropores and pinhole-like macrospaces here) (section 3.3). The presence of pinhole-like macrospaces in the film is significant for retaining the mesostructural ordering after full crystallization during calcination at 400 °C. Expansion of pinhole-like macrospaces during calcination (Fig. 10) would offset the tensile stress by shrinkage with complete crystallization of the titania frameworks on the substrate, and thus ordered mesoporous anatase films can be prepared using commercially available and frequently used Pluronic surfactants in the aqueous system.

Emulsion-induced macropores and pinhole-like macrospaces are not uniform (Fig. 9 and 10) and the pore sizes are not controllable, so their role was investigated more clearly by the addition of uniform PS beads instead of TIPBz. When aqueous solutions of polystyrene (PS) beads with diameters of 100 nm and 300 nm were added to the precursor solution, macropores derived from the PS beads shrank to *ca.* 80 nm and *ca.* 250 nm, respectively, in mesoporous titania films calcined at 400 °C. PS beads with diameters of 900 nm, larger than the film thickness, resulted in as-made and calcined films as shown in Fig. 11, with the corresponding TEM image of the as-made film. The TEM image of the as-made film exactly showed the presence of

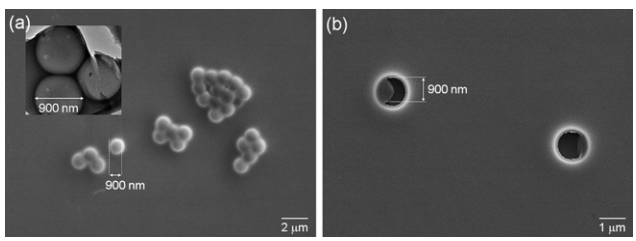

Fig. 11 SEM images of (a) as-made and (b) calcined (at 400 °C) films prepared using F127 in the presence of PS beads (900 nm) with (inset) the TEM image of the as-made film.

uniform macropores with the diameter of 900 nm. The diameter of PS-derived holes was larger than 900 nm after calcination at 400 °C, indicating expansion of macropores. Therefore, the additional experiment also supports that expansion of pinhole-like macrospaces is important for the retention of ordered mesostructures during full crystallization of titania frameworks.

3.5 Adsorption of DNA molecules over mesoporous titania films

The adsorbed amounts of DNA molecules over mesoporous titania films calcined at 250 and 400 °C and films composed of P25 are shown in Fig. 12. Many DNA molecules can be adsorbed over mesoporous titania films calcined at 400 °C. However, the DNA molecules cannot be accommodated in the ordered mesopores because the size of the DNA molecule is around 10 nm larger than the mesopores. Accordingly, it is considered that the amount of macropores in the mesoporous anatase film influences the adsorbed amount of the large DNA molecules, as shown in Scheme 2. In addition, the DNA molecules did not adsorb over the mesoporous titania film calcined at 250 °C, though the film also contained such macropores. The result reveals that adsorption of the DNA molecules is related to not only the presence of macropores but also the crystallinity of the titania frameworks. In the case of the P25 films, the thickness was not dependent on the adsorbed amount of DNA molecules, suggesting that the DNA molecules cannot adsorb inside the P25 films and only adsorb at the surfaces. Nevertheless, the adsorbed amount of DNA molecules was larger than that adsorbed over the mesoporous titania film calcined at 250 °C. The result also supports the conclusion that adsorption of DNA molecules is related to the crystallinity of titania frameworks, which is important for practical use of the completely crystallized mesoporous titania films containing macropores in photoelectric nano-devices.

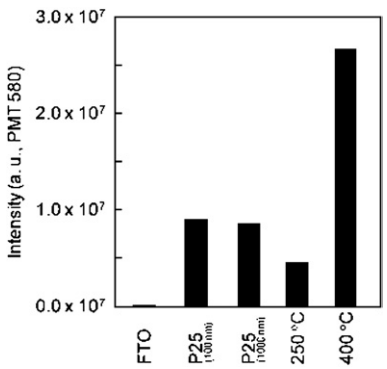

Fig. 12 Adsorption amounts of DNA molecules over mesoporous titania films calcined at 250 °C and 400 °C, compared with those over a FTO substrate and P25 films with different thicknesses.

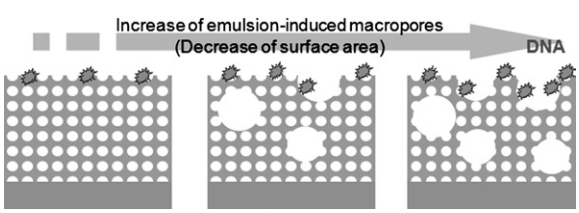

Scheme 2 Schematic formation mechanism of semi-crystalline mesoporous titania film containing macropores.

4. Conclusions

An ordered mesoporous titania film with strongly enhanced crystallinity was successfully prepared using commercially available and frequently used Pluronic surfactants in an aqueous system containing organic additives, leading to the formation of emulsion-induced macropores and anatase nanoparticles. The use of a water-soluble triblock copolymer such as Pluronic F127 allows the synthesis in the aqueous system, which will subsequently lead to further design of mesostructured and mesoporous titania films using soluble organic dyes and organometallic complexes for potential uses in dye-sensitized solar cells and highly selective adsorbents including biocatalysts. The enhanced crystallinity influenced the adsorption behavior of DNA molecules over porous titania films. These insights will widely contribute to the development of novel applications of hierarchical mesoporous–macroporous titania films to optics, sensors, photocatalysts, and electronics, including gene delivery materials.

Acknowledgements

This work is supported by the Ministry of Economy, Trade and Industry (METI), Japan, as a part of the Environmentally Friendly Sensor Project. We acknowledge Drs Shuji Sonezaki, Hitoshi Ohara, Makoto Bekki, and Yoshimasa Yamane (TOTO Ltd.) for kind cooperation and helpful discussions to investigate adsorption properties of DNA molecules.

References

1 G. J. A. A. Soler-Illia, C. Sanchez, B. Lebeau and J. Patarin, *Chem. Rev.*, 2002, **102**, 4093.
2 Y. Wan and D. Zhao, *Chem. Rev.*, 2007, **107**, 2821.
3 B. Tian, X. Liu, B. Tu, C. Yu, J. Fan, L. Wang, S. Xie, G. D. Stucky and D. Zhao, *Nat. Mater.*, 2003, **2**, 159.
4 C. Yu, B. Tian and D. Zhao, *Curr. Opin. Solid State Mater. Sci.*, 2003, **7**, 191.
5 N. Bai, S. Li, H. Chen and W. Pang, *J. Mater. Chem.*, 2001, **11**, 3099.
6 Y. K. Hwang, K.-C. Lee and Y.-U. Kwon, *Chem. Commun.*, 2001, 1738.
7 K.-S. Jang, M.-G. Song, S.-H. Cho and J.-D. Kim, *Chem. Commun.*, 2004, 1514.
8 D. Grosso, G. J. A. A. Soler-Illia, F. Babonneau, C. Sanchez, P.-A. Albouy, A. Brunet-Bruneau and A. R. Balkenende, *Adv. Mater.*, 2001, **13**, 1085.
9 E. L. Crepaldi, G. J. A. A. Soler-Illia, D. Grosso, F. Cagnol, F. Ribot and C. Sanchez, *J. Am. Chem. Soc.*, 2003, **125**, 9770.
10 E. L. Crepaldi, G. J. de A. A. Soler-Illia, D. Grosso and C. Sanchez, *New J. Chem.*, 2003, **27**, 9.
11 M. Etienne, D. Grosso, C. Boissière, C. Sanchez and A. Walcarius, *Chem. Commun.*, 2005, 4566.
12 P. C. A. Alberius, K. L. Frindell, R. C. Hayward, E. J. Kramer, G. D. Stucky and B. F. Chmelka, *Chem. Mater.*, 2002, **14**, 3284.
13 K. L. Frindell, M. H. Bartl, A. Popitsch and G. D. Stucky, *Angew. Chem., Int. Ed.*, 2002, **41**, 960.
14 N. Bao, K. Yanagisawa, X. Lu and X. Feng, *Chem. Lett.*, 2004, **33**, 346.
15 K. Liu, M. Zhang, K. Shi and H. Fu, *Mater. Lett.*, 2005, **59**, 3308.

16 S. Y. Choi, B. Lee, D. B. Carew, M. Mamak, F. C. Peiris, S. Speakman, N. Chopra and G. A. Ozin, *Adv. Funct. Mater.*, 2006, **16**, 1731.
17 J. C. Yu, X. Wang and X. Fu, *Chem. Mater.*, 2004, **16**, 1523.
18 B. L. Kirsch, E. K. Richman, A. E. Riley and S. H. Tolbert, *J. Phys. Chem. B*, 2004, **108**, 12698.
19 K. Wang, M. A. Morris and J. D. Holmes, *Chem. Mater.*, 2005, **17**, 1269.
20 K. Wang, B. Yao, M. A. Morris and J. D. Holmes, *Chem. Mater.*, 2005, **17**, 4825.
21 K. M. Coakley, Y. Liu, M. D. McGehee, K. L. Frindell and G. D. Stucky, *Adv. Funct. Mater.*, 2003, **13**, 301.
22 Y. Sakatani, D. Grosso, L. Nicole, C. Boissière, G. J. de A. A. Soler-Illia and C. Sanchez, *J. Mater. Chem.*, 2006, **16**, 77.
23 Y. Segura, L. Chmielarz, P. Kustrowski, P. Cool, R. Dziembaj and E. F. Vansant, *J. Phys. Chem. B*, 2006, **110**, 948.
24 M. A. Carreon, S. Y. Choi, M. Mamak, N. Chopra and G. A. Ozin, *J. Mater. Chem.*, 2007, **17**, 82.
25 Y. Zhang, J. Li and J. Wang, *Chem. Mater.*, 2006, **18**, 2917.
26 W. Ho, J. C. Yu and S. Lee, *Appl. Catal. B*, 2007, **73**, 135.
27 S. S. Soni, M. J. Henderson, J.-F. Bardeau and A. Gibaud, *Adv. Mater.*, 2008, **20**, 1493.
28 E. Allain, S. Besson, C. Durand, M. Mélanie, T. Gacoin and J.-P. Boilot, *Adv. Funct. Mater.*, 2007, **17**, 549.
29 L. Malfatti, P. Falcaro, H. Amenitsch, S. Caramori, R. Argazzi, C. A. Bignozzi, S. Enzo, M. Maggini and P. Innocenzi, *Micropor. Mesopor. Mater.*, 2006, **88**, 304.
30 E. Lancelle-Beltran, P. Prené, C. Boscher, P. Belleville, P. Buvat and C. Sanchez, *Adv. Mater.*, 2006, **18**, 2579.
31 M. Wei, K. Wang, M. Yanagida, H. Sugihara, M. A. Morris, J. D. Holmes and H. Zhou, *J. Mater. Chem.*, 2007, **17**, 3888.
32 J. Procházka, L. Kavan, V. Shklover, M. Zukalová, O. Frank, M. Kalbáč, A. Zukal, H. Pelouchová, P. Janda, K. Mocek, M. Klementová and D. Carbone, *Chem. Mater.*, 2008, **20**, 2985.
33 Z. Qi, I. Honma and H. Zhou, *J. Phys. Chem. B*, 2006, **110**, 10590.
34 D. Grosso, G. J. A. A. Soler-Illia, E. L. Crepaldi, F. Cagnol, C. Sinturel, A. Bourgeois, A. Brunet-Bruneau, H. Amenitsch, P. A. Albouy and C. Sanchez, *Chem. Mater.*, 2003, **15**, 4562.
35 J. D. Bass, D. Grosso, C. Boissiere and C. Sanchez, *J. Am. Chem. Soc.*, 2008, **130**, 7882.
36 B. Smarsly, D. Grosso, T. Brezesinski, N. Pinna, C. Boissière, M. Antonietti and C. Sanchez, *Chem. Mater.*, 2004, **16**, 2948.
37 D. Fattakhova-Rohlfing, M. Wark, T. Brezesinski, B. Smarsly and J. Rathouský, *Adv. Funct. Mater.*, 2007, **17**, 123.
38 W. Chen, Y. Geng, X.-D. Sun, Q. Cai, H.-D. Li and D. Weng, *Micropor. Mesopor. Mater.*, 2008, **111**, 291.
39 C.-W. Wu, T. Ohsuna, M. Kuwabara and K. Kuroda, *J. Am. Chem. Soc.*, 2006, **128**, 4544.
40 C.-W. Koh, U.-H. Lee, J.-K. Song, H.-R. Lee, M.-H. Kim, M. Suh and Y.-U. Kwon, *Chem. Asian J.*, 2008, **3**, 862.
41 Y. Zhang, J. Li and J. Wang, *Chem. Mater.*, 2006, **18**, 2917.
42 M. Cecilia and G. J. A. A. Soler-Illia, *Chem. Mater.*, 2006, **18**, 2109.
43 P. C. Angelomé, M. C. Fuertes and G. J. A. A. Soler-Illia, *Adv. Mater.*, 2006, **18**, 2397.
44 B. T. Holland, C. F. Blanford and A. Stein, *Science*, 1998, **281**, 538.
45 B. T. Holland, C. F. Blanford, T. Do and A. Stein, *Chem. Mater.*, 1999, **11**, 795.
46 J. E. G. J. Wijnhoven and W. L. Vos, *Science*, 1998, **281**, 803.
47 A. Imhof and D. J. Pine, *Nature*, 1997, **389**, 948.
48 K. L. Frindell, M. H. Bartl, M. R. Robinson, G. C. Bazan, A. Popitsch and G. D. Stucky, *J. Solid State Chem.*, 2003, **172**, 81.
49 K. L. Frindell, J. Tang, J. H. Harreld and G. D. Stucky, *Chem. Mater.*, 2004, **16**, 3524.
50 J. C. Yu, X. Wang, L. Wu, W. Ho, L. Zhang and G. Zhou, *Adv. Funct. Mater.*, 2004, **14**, 1178.
51 E. Martinez-Ferrero, D. Grosso, C. Boissière, C. Sanchez, O. Oms, D. Leclercq, A. Vioux, F. Miomandre and P. Audebert, *J. Mater. Chem.*, 2006, **16**, 3762.
52 E. Lancelle-Beltran, P. Prené, C. Boscher, P. Belleville, P. Buvat, S. Lambert, F. Guillet, C. Boissière, D. Grosso and C. Sanchez, *Chem. Mater.*, 2006, **18**, 6152.
53 Y. Zhang, A. H. Yuwono, J. Li and J. Wang, *Micropor. Mesopor. Mater.*, 2008, **110**, 242.
54 Y. Liu, X. Wang, F. Yang and X. Yang, *Micropor. Mesopor. Mater.*, 2008, **114**, 431.
55 S. Hudson, J. Cooney and E. Magner, *Angew. Chem., Int. Ed.*, 2008, **47**, 8582.
56 C. Yu, B. Tian, J. Fan, G. D. Stucky and D. Zhao, *J. Am. Chem. Soc.*, 2002, **124**, 4556.
57 D. Li, Y. Han, J. Song, L. Zhao, X. Xu, Y. Di and F.-S. Xiao, *Chem. Eur. J.*, 2004, **10**, 5911.
58 P. I. Ravikovitch and A. V. Neimark, *Langmuir*, 2002, **18**, 9830.
59 F. Kleitz, D. Liu, G. M. Anilkumar, I.-S. Park, L. A. Solovyov, A. N. Shmakov and R. Ryoo, *J. Phys. Chem. B*, 2003, **107**, 14296.
60 K. Morishige and M. Ishino, *Langmuir*, 2007, **23**, 11021.
61 M. Kruk, V. Antochshuk, J. R. Matos, L. P. Mercuri and M. Jaroniec, *J. Am. Chem. Soc.*, 2002, **124**, 768.
62 V. Antochshuk, M. Kruk and M. Jaroniec, *J. Phys. Chem. B*, 2003, **107**, 11900.

